Environmental Science
Water Research & Technology

Photodegradation of pharmaceutical compounds in partially nitritated wastewater during UV irradiation

Journal:	*Environmental Science: Water Research & Technology*
Manuscript ID	EW-ART-10-2018-000714.R1
Article Type:	Paper
Date Submitted by the Author:	26-Feb-2019
Complete List of Authors:	Hora, Priya; University of Minnesota, Civil, Environmental, and Geo-Engineering Novak, Paige; University of Minnesota, Arnold, William; University of Minnesota, Civil Engineering

Water impact statement

Incorporating an ultraviolet photolysis step during partial biological nitritation could be used to enhance the transformation of pharmaceuticals found in municipal wastewater through the generation of hydroxyl radicals via nitrite photolysis. Formation of nitrogenous disinfection byproducts, however, could be a concern.

Photodegradation of pharmaceutical compounds in partially nitritated wastewater during UV irradiation‡

Priya I. Hora, Paige J. Novak, and William A. Arnold*

Department of Civil, Environmental, and Geo- Engineering, University of Minnesota – Twin Cities, 500 Pillsbury Drive SE, Minneapolis, Minnesota 55455, United States

*Author to whom correspondence should be addressed. Phone: 612-625-8582; Fax: 612-626-7750; email: arnol032@umn.edu

Footnote

‡Electronic Supplementary Information (ESI) available.

Abstract

The first step of an anaerobic ammonia oxidation (anammox) system is typically the formation of nitrite (NO_2^-) via partial nitritation, which can generate hydroxyl radical ($^{\bullet}OH$) when irradiated with ultraviolet (UV) light. This study demonstrated that the presence of nitrite in buffer and wastewater matrices during medium-pressure UV irradiation (at $\lambda \geq 220$ or ≥ 280 nm) enhanced the degradation of select pharmaceutical compounds of different therapeutic classes (atenolol, carbamazepine, fluoxetine, and trimethoprim). Total pharmaceutical removals in a wastewater matrix irradiated at $\lambda \geq 280$ for 120 minutes were 47% for trimethoprim, 50% for carbamazepine, 60% for atenolol, and 57% for fluoxetine at fluences of 58.6 mEi m^{-2} (2033.1 mJ cm^{-2}). When irradiated at $\lambda \geq 220$ for 60 minutes, removals were 52% for trimethoprim, 56% for carbamazepine, 69% for atenolol, and 90% for fluoxetine at fluences of 634.7 mEi m^{-2} (23969.2 mJ cm^{-2}). Reaction with $^{\bullet}OH$ accounted for ~78 – 90% of pharmaceutical removal at $\lambda \geq 280$ nm. Although direct photolysis did contribute to target compound removal for irradiation with $\lambda \geq 220$ nm, much of the light was absorbed in the buffer and wastewater matrices, and reaction with $^{\bullet}OH$ accounted for ~70 – 93% of pharmaceutical removal. Quencher experiments with isopropanol confirmed the importance of reaction with $^{\bullet}OH$ as the main contributor to pharmaceutical removal. *para*-Chlorobenzoic acid was used as a probe to estimate steady-state $^{\bullet}OH$ concentrations, which averaged 8.58×10^{-15} M for both matrices at $\lambda \geq 280$ nm and 3.50×10^{-14} M for both matrices at $\lambda \geq 220$ nm. Nitrosamines were formed and accumulated during the UV treatment step, however, concomitant with their direct photochemical destruction. Presence of the pharmaceutical micro-pollutants studied, such as the secondary-amine containing atenolol and fluoxetine, did not elevate nitrosamine formation.

Introduction

Contaminants of emerging concern (CECs) are common household and industrial chemicals that have been detected in wastewater treatment plant effluent and effluent-impacted water bodies.[1,2] In wastewater treatment, biological processes such as conventional activated sludge are commonly used, but were not specifically designed for the removal of CECs.[2,3] Pharmaceuticals and personal care products are amongst the myriad of potentially recalcitrant, unregulated CECs that are detected in effluent and the environment.[1,4] Of the pharmaceuticals detected in wastewater effluent and surface water, beta-blockers, antidepressants, antibiotics, and the antiepileptic carbamazepine are some of the most studied because they are highly prescribed, ubiquitous in wastewater influent, and exhibit variable susceptibility to biological removal, with carbamazepine considered particularly recalcitrant.[1–3,5] As a result, these compounds have been frequently detected in wastewater effluent at nanogram to microgram per liter concentrations.[1–3,6] Several pharmaceuticals, including carbamazepine and trimethoprim, have also shown a degree of persistence in the environment, with photolysis being identified over biodegradation and hydrolysis as an important loss mechanism in sunlight-exposed surface water.[7–11] Consequently, the use of photolysis for treatment of CECs has generated interest.[12–18]

Because conventional wastewater treatment processes are energy intensive, a shift is occurring towards energy neutral treatment and re-envisioning wastewater as a renewable resource with the potential for energy recovery.[19] One way in which this re-envisioning is taking place is through the replacement of energy-intensive conventional biological nitrogen removal (BNR) (nitrification-denitrification) with partial-nitritation/anammox (PN/A), in which ammonia is first partially biologically oxidized to nitrite, followed by a second anaerobic

biological ammonia oxidation step to nitrogen gas, in which ammonium serves as the electron donor and nitrite is the electron acceptor.[20–23] The use of PN/A leads to an estimated 25% to 60% reduction in aeration requirements, with resulting reductions in energy use.[19,22–24] There is evidence for biological removal of CECs during PN/A treatment,[25–27] but an opportunity might exist to combine PN/A with chemical treatment to provide more complete CEC removal.

In aqueous systems at environmentally relevant pH values, nitrite is known to absorb UV light in the 200 to 400 nm range and produce hydroxyl radical ($^{\bullet}OH$; quantum yield 0.024-0.078, compared to 0.007 – 0.014 for nitrate[28]), a non-selective and highly reactive species that oxidizes organic contaminants.[29–32] Many trace organic contaminants have been effectively removed by advanced oxidation processes (AOPs) that generate $^{\bullet}OH$.[16,18,33,34] For example, carbamazepine, atenolol, fluoxetine, and trimethoprim are all known to be degraded via reaction with $^{\bullet}OH$.[8,11,12,16,18,35] In systems containing nitrite, such as a system in which partial nitritation has taken place, a UV disinfection step could be leveraged to generate a de facto AOP using constituents in the wastewater[13] prior to the second anammox step, especially because nitrite is a more efficient producer of hydroxyl radical compared to nitrate.

While production of reactive radical species, such as hydroxyl radical, from nitrite and nitrate photolysis has been extensively studied in sunlit natural waters,[9,29,30,36–40] much of the work investigating the relevance of this phenomenon to contaminant degradation with regard to water and wastewater treatment processes has focused on the impact of *nitrate* during UV or sunlight photolysis.[12,13,17,41–43] Many of the referenced studies looking at contaminant degradation in effluent have focused on *nitrified* wastewater. Rosario-Ortiz et al.[16] briefly touch on the influence of nitrite in their study of pharmaceutical oxidation in wastewater (by UV/H_2O_2), but only in terms of its hydroxyl radical scavenging capacity. Bahnmüller et al.[44]

88 attribute a percentage of antibiotic transformation in effluents to hydroxyl radical generated by
89 the photolysis of nitrite. Their experiments, however, were conducted using a solar simulator or
90 a medium pressure mercury lamp transmitting $\lambda > 320$ nm. In their study on medium pressure
91 UV disinfection of nitrified effluents, Keen et al.[13] determined both the quantum yield for $^{\bullet}OH$
92 formation from nitrite at $\lambda < 240$ nm and the steady-state hydroxyl radical concentrations
93 produced because there is a synergistic effect wherein nitrate photolysis can generate nitrite,
94 which photolyzes to produce additional $^{\bullet}OH$. It should also be noted that the NO_2^-
95 concentrations in the aforementioned studies were below 1 mg/L-N. The study presented herein
96 is the first to investigate the steady-state concentration of hydroxyl radical produced by nitrite
97 and subsequent degradation of several organic contaminants in *nitritated* wastewater, that is
98 water with appreciable levels of nitrite (e.g., around 20 mg/L-N), when irradiated by a medium
99 pressure mercury vapor lamp at shorter wavelength ranges. The results of this study are all the
100 more important because it was previously concluded that UV photolysis of NO_2^- would not be a
101 viable advanced oxidation technology.[29]

102 Nevertheless, one concern with this strategy is formation of nitrosamines from nitrite or
103 pharmaceutical compounds containing secondary amines.[45–49] Photonitrosation of natural
104 organic matter can occur after medium pressure UV irradiation of nitrite.[50] One nitrosamine, N-
105 nitrosodimethylamine (NDMA), reportedly forms photochemically in the presence of nitrite via
106 nitrosation, though NDMA is also subsequently and rapidly degraded
107 photochemically.[29,45,47,51–53] It has also been hypothesized that amine-containing
108 pharmaceuticals can serve as important sources of NDMA precursors in domestic
109 sewage.[45,48,51] There has been no work, however, identifying and attributing the relative

importance of specific constituents for nitrosamine formation during UV treatment of wastewater effluent.

In this study, the prospect of implementing UV irradiation in between partial nitritation and annamox processes as a potential means for enhancing removal of pharmaceuticals was evaluated. The compounds selected for study, carbamazepine, trimethoprim, fluoxetine, and atenolol, are regularly prescribed and have been routinely detected in wastewater effluents, receiving water bodies, and drinking water supplies[54–56] and are neither readily biodegraded nor destroyed rapidly by solar direct photolysis. It was hypothesized that the nitrite in solution would efficiently generate $^{\bullet}OH$ and lead to transformation of contaminants via indirect photolysis. The possibility of photochemical nitrosamine formation from both nitrite and the pharmaceuticals themselves was assessed, and a kinetic model was developed that factored in both formation and destruction of NDMA by UV to evaluate nitrosamine concentration under different worst-case scenarios.

Materials and Methods

Chemicals and reagents

All pharmaceutical compounds used in this study were reagent or analytical grade (≥ 98% pure) and used as received: carbamazepine (Acros Organics), trimethoprim (Acros Organics), fluoxetine hydrochloride (TCI America), and atenolol (Sigma-Aldrich). Structures are shown in Table S1. Aqueous stocks and solutions were prepared using ultrapure water (resistivity 18.2 MΩ-cm, Millipore Corp). *para*-Chlorobenzoic acid (pCBA; Acros Organics) was used as a hydroxyl radical probe.[57] Sodium nitrite (>95%, Fisher) and ammonium sulfate (≥99%, Sigma-Aldrich) salts were added to adjust the concentrations of desired nitrogen species

133 in experimental solutions. Atrazine (99.8%, Fluka) was used as an actinometer.[58] High pressure
134 liquid chromatography (HPLC) grade isopropanol (IPA; 99.9%, Fisher) was used as a radical
135 quencher. HPLC grade acetonitrile (99.9%, Fisher) was used in HPLC eluents.
136
137 *Reactor effluent collection and processing*
138 Wastewater effluent was collected from a 5-L bench-scale biological sequencing batch
139 reactor operated under conditions favorable to anammox, fed a synthetic nitrite- and ammonium-
140 rich influent, and seeded with sludge from a full-scale DEMON system (York River wastewater
141 treatment plant, Seaside, VA).[27] The effluent was collected in a clean plastic container over one
142 complete pump-out cycle from the reactor and was stored overnight in the dark at 4 °C until
143 further processing and analysis the following day. The effluent was transferred to four 250-mL
144 sterile Corning centrifuge tubes and centrifuged at 5,000 rpm for 35 minutes at 2 °C. The
145 supernatant was then vacuum filtered; first, through 0.7-µm pre-combusted glass fiber filters to
146 remove larger solids and particulate matter and then through a 0.2-µm Omnipore membrane filter
147 (Millipore). The filtered effluent was subsequently analyzed for anions, ammonium, dissolved
148 organic carbon (DOC), dissolved inorganic carbon (DIC), and pH, then stored at 4 °C in the dark
149 until use. The reactor effluent water quality measurements are provided in Table S2.
150
151 *Experimental set-up*
152 **Photolysis Experiments.** Photolysis experiments with individual compounds were
153 performed in duplicate in ultrapure water and two nitrogen-containing matrices: (1) a carbon-free
154 synthetic wastewater matrix containing sodium nitrite and ammonium sulfate at approximately
155 20 mg-N/L each (referred to as "synthetic nitrogen-containing matrix") and (2) the wastewater

156 matrix to which additional sodium nitrite and ammonium sulfate were added to reach
157 approximately 20 mg-N/L of each nitrogen species (referred to as "nitrogen-containing
158 wastewater matrix"). These ammonium and nitrite concentration levels were selected as a
159 reasonable amount to expect from an actual partial-nitritation preparatory step based on a range
160 of ammonium values found in effluent from studies on anaerobic treatment of domestic
161 wastewater (9 – 67 mg of N/L)[24] and typical partial nitritation stoichiometry.[20,59,60] The ultrapure
162 water and "synthetic nitrogen-containing matrix" solutions were buffered (5 mM phosphate
163 buffer, pH 7.5) to match the pH of the wastewater reactor effluent (reported in Table S2).
164 The extent of pharmaceutical degradation in these systems was assessed by tracking loss
165 of the parent compound under two UV irradiation conditions. Pharmaceuticals were amended
166 from concentrated aqueous stock solutions (prepared in unbuffered ultrapure water) to achieve a
167 concentration of approximately 1 μM. The initial pharmaceutical concentration was selected to
168 be high enough to ensure adequate detection and quantification during the course of the
169 experiment and low enough so as not to contribute significantly to background radical
170 scavenging or light screening.
171 Test solutions were irradiated in capped quartz test tubes (V=10 mL, i.d.= 1.1 cm, o.d.=
172 1.3 cm)[17,61] with a 450-W medium-pressure mercury vapor lamp (Ace Glass Inc., Vineland NJ)
173 emitting polychromatic light. The lamp was situated in a quartz immersion well with tap water
174 circulation. Samples were placed in a merry-go-round equipped with a fan for temperature
175 control, which rotated around the lamp. The lamp was warmed up for at least 10 minutes prior to
176 sample irradiation to ensure full, steady power output. Steady output was confirmed on two
177 occasions using a broadband PMA2100 radiometer with PMA2110-WP (UVA) and PMA2106-
178 WP (UVB) detectors. Either a quartz ($\lambda \geq 220$ nm) or Pyrex ($\lambda \geq 280$ nm) cutoff filter sleeve was

179 used for experiments. Control experiments to account for direct photolysis consisted of spiking
180 the pharmaceutical compounds into buffered ultrapure water without nitrite or ammonium.
181 Control experiments to account for non-photochemical losses were also performed in which the
182 test tubes were wrapped in aluminum foil. Sub-samples from all test tubes were withdrawn at
183 regular time intervals using pre-combusted glass Pasteur pipettes and the concentration of the
184 pharmaceuticals was measured.

185 Pseudo first-order reaction rate constants were derived from the slopes determined by
186 linear regression of natural log concentration versus time plots of the data. The 95% confidence
187 intervals for each rate constant were calculated by multiplying the standard error of the slope
188 from Excel's LINEST function by the results of the two-tailed inverse of the Student's t-
189 distribution (T.INV.2T function in Excel).

190 To test for nitrosamine formation, six 50-mL aliquots of the nitrogen-containing
191 wastewater effluent with a molar concentration of approximately 9.92×10^{-4} M nitrite were
192 apportioned out for total N-nitrosamine (TONO) formation experiments. Half of the aliquots
193 were spiked with a cocktail of pharmaceuticals (1 μM of each). Duplicate samples were
194 irradiated in borosilicate test tubes with the 280 nm cutoff in place or in quartz test tubes with the
195 220 nm cutoff. A dark control wrapped in aluminum foil was also irradiated for each condition.
196 Samples were exposed for 2 hours with the aim of achieving pharmaceutical degradation to at
197 least two half-lives. Samples were stored at 4 °C in glass bottles prior to being shipped on ice to
198 Syracuse University.

199 **Lamp fluence measurement.** Chemical actinometry was used to characterize the UV
200 dose or fluence of the lamp. The incident photon fluence rate value or incident photon irradiance,
201 E_p^0, in the wavelength intervals from 220 nm or 280 nm to 405 nm (because nitrite absorbs deep

UV (λ<240 nm) as well as wavelengths up to 400 nm[13]) was determined at low optical density using 9 μM aqueous atrazine, buffered at pH 7.0 in 10 mM phosphate buffer, as an actinometer[58,62,63]. Identical geometry and similar solution volumes were used as in the photolysis experiments. Per Canonica et al.,[58] using the spectral energy distribution of radiated mercury lines provided by the lamp manufacturer, and assuming negligible light absorbance or attenuation over the depth of the solution, the fluence was calculated according to:

$$E^0_{p(\lambda_1 - 405\ nm)} = \frac{k_{p,atr}}{2.303\phi_{atr}\Sigma_{\lambda_1}^{405\ nm}(f_{p,\lambda}\varepsilon_{atr,\lambda})} \quad (1)$$

where $\lambda_1 = 220\ or\ 280\ nm,\ k_{p,atr}$ is the pseudo first-order rate of atrazine degradation, ϕ_{atr} is the quantum yield of atrazine degradation ($0.046\ mol\ Ei^{-1}$) assuming wavelength independence, $f_{p,\lambda}$ is the photon flux-based emission spectrum of the lamp normalized over the wavelength interval, and $\varepsilon_{atr,\lambda}$ is the molar absorption coefficient of atrazine. Because the experiment was performed in buffered Milli-Q water, and the solute concentration was relatively low, it was assumed that negligible light absorption (i.e., α×z < 0.02, where α is the light attenuation coefficient and z is solution depth) occurred, allowing the use of the near-surface approximation. The incident photon fluence rate values (E^0_p) were determined to be $176.3\ \mu Ei\ m^{-2}s^{-1}$ ($6.7\ mJ\ cm^{-2}s^{-1}$) and $8.1\ \mu Ei\ m^{-2}s^{-1}$ ($0.3\ mJ\ cm^{-2}s^{-1}$) for 220 – 405 nm and 280 – 405 nm, respectively. UV fluence values reported below are calculated by using the appropriate E_p^0 value multiplied by the exposure time.

Quantification of hydroxyl radical concentrations. The steady-state hydroxyl radical concentration ($[^{\bullet}OH]_{ss}$) was calculated from the disappearance of 5 μM of the radical-specific molecular probe compound pCBA in the nitrogen-containing matrices irradiated under the same conditions as the pharmaceuticals. It is also possible that reactive nitrogen species such as $NH_2^{\bullet}$, $NO^{\bullet}$, and $NO_2^{\bullet}$ could form in these systems.[29,31,64] Evidence suggests, however, that these species

are less potent oxidants than hydroxyl radical. Reactivity between pCBA or benzoate ion has not been reported for $NO_2^{\bullet}$ or $NO^{\bullet}$. $NH_2^{\bullet}$ does not appear to react quickly with benzoate ion (k <1x10^5 M^{-1} s^{-1} at pH 11.2).[65]

A direct photolysis control of the probe compound in buffered ultrapure water was also performed. If pCBA concentration is sufficiently low so as not to affect $[^{\bullet}OH]_{ss}$, the rate of pCBA loss is proportional to the $^{\bullet}OH$ concentration, and follows pseudo first-order kinetics:

$$\frac{d[pCBA]}{dt} = -k'_{pCBA}[pCBA] \quad (2)$$

$$k'_{pCBA} = k_{\cdot OH,pCBA}[\cdot OH]_{ss} \quad (3)$$

Rate constants (k') were determined as described above. The second-order scavenging rate constant for reaction of pCBA with $^{\bullet}OH$ is $k_{\bullet OH,pCBA} = 5 \times 10^9$ M^{-1}s^{-1}.[66] Thus, $[^{\bullet}OH]_{ss} = k'_{pCBA}/k_{\bullet OH,pCBA}$. For $\lambda \geq 280$ nm, direct photolysis rates were subtracted to ascertain the indirect contribution. The overall pseudo first-order photolysis rate constant for compound loss in the nitrogen-containing matrices is $k'_{nitrogen-containing}$ and the indirect photolysis pseudo first-order rate constant is $k'_{indirect,280} = k'_{nitrogen-containing} - k'_{direct}$, where $k'_{direct}$is the direct photolysis pseudo first-order rate constant of the compound in buffer.

To assess and account for any direct photochemical losses of pCBA in the nitrite-containing matrices for $\lambda \geq 220$ nm, 1% IPA, a $^{\bullet}OH$ quencher,[12,17,61] was added to determine the role of indirect versus direct photolysis of the probe. If IPA dramatically suppresses the reaction, it would indicate that direct photolysis reactions are limited due to light screening by the nitrite or other matrix components, and loss of pCBA in the unquenched samples was due to interaction with $^{\bullet}OH$. Thus, the decrease in the pseudo first-order rate constant resulting from the quenching of $^{\bullet}OH$ in the nitrogen-containing synthetic and wastewater matrices would be equivalent to the contribution of $^{\bullet}OH$ to overall photolysis of the probe (i.e., $k'_{indirect,220} = k'_{nitrogen-containing} -$

$k'_{nitrogen-containing,IPA}$) as distinct from direct photolysis, allowing for an upper bound estimate of steady-state hydroxyl radical concentration. Equation 4 shows the calculation for steady-state hydroxyl radical concentration for $\lambda \geq 220$ nm.

$$[\cdot OH]_{ss,220} = k'_{indirect,220} / k_{\cdot OH,pCBA} \quad (4)$$

Experimental bimolecular rate constants for reaction of each pharmaceutical with •OH could be determined using the calculated steady-state •OH concentrations and the pseudo first-order rate constants for pharmaceutical loss, as shown in equation 5:

$$k_{OH,Pharm} = \frac{k'_{indirect}}{[\cdot OH]_{ss}} \quad (5)$$

Indirect photolysis contribution to pharmaceutical loss. The indirect photolysis contribution in the two nitrogen-containing matrices was estimated using equation 6 and the respective $k'_{indirect}$ values for each pharmaceutical at $\lambda \geq 220$ nm and 280 nm.

$$\%\ indirect = \frac{k'_{indirect}}{k'_{nitrogen-containing}} \times 100 \quad (6)$$

Analytical methods

Water quality parameters. Anions (nitrate and nitrite) were measured by ion chromatography using a Metrohm Compact ion chromatograph. Combined nitrite and nitrate standards made with sodium salts were also run to generate calibration curves. Ammonium (measured as ammonia) was measured colorimetrically using a Hach Test 'N Tube™ kit (AmVer™ High Range Ammonia Reagent Set 2606945, Method 10031, Hach Corporation) and a Hach DR 900 colorimeter. Dissolved organic carbon (DOC), as non-purgeable organic carbon, and dissolved inorganic carbon (DIC) were measured with a Shimadzu TOC-L total organic carbon analyzer. Calibration curves were generated using potassium hydrogen phthalate for DOC and anhydrous sodium carbonate and sodium bicarbonate for DIC. Reactor effluent pH was

measured using a calibrated Thermo Orion pH probe and Thermo Orion DUAL STAR pH/ISE meter (pH 4, 7, and 10 standard solutions from BDH VWR Analytical).

Absorption spectra. Light absorbance of the matrices and buffered aqueous pharmaceutical, pCBA, and actinometer solutions at the same concentration used in experiments (1-9 μM) were measured with a Shimadzu UV-1601PC spectrophotometer using 1 cm quartz cuvettes (Figure S1).

Measurement of pharmaceutical compounds, pCBA, and atrazine. Sub-samples were dispensed into 200 μL HPLC vial inserts. Losses of the pharmaceutical compounds, atrazine, and pCBA were measured using an Agilent 1100 HPLC equipped with a UV absorbance detector. Isocratic HPLC methods are summarized in the Electronic Supplementary Information (Table S3).

Nitrosamine quantification. TONO analysis followed protocols described previously.[48,67,68] Details are provided in the ESI.

Results and Discussion

Reactions driven by $^{\bullet}$OH in nitrogen-containing wastewater matrices at $\lambda \geq 280$ nm

pCBA degradation was used to determine the steady state concentration of $^{\bullet}$OH produced from the photolysis of the nitrogen-containing matrices at $\lambda \geq 280$ nm. pCBA degradation was pseudo first-order for $\lambda \geq 280$ conditions (Figure 1A), demonstrating that $^{\bullet}$OH formed in the nitrogen-containing matrices at fluences up to 73.2 mEi m^{-2}. The kinetics in both the nitrogen-containing synthetic matrix and wastewater were very similar (Table S4a), suggesting that nitrite was responsible for $^{\bullet}$OH production. The calculated steady-state $^{\bullet}$OH concentrations are reported in Table 1, and were similar to those measured by Keen et al.,[13] despite significantly higher

293 nitrite concentrations in our system (20 mg/L as N compared to ~0.6 mg/L as N resulting in an
294 $[^{\bullet}OH]_{ss} \approx 3.25\times10^{-14}$ M[13]). Carbonate species, DOC, and ammonium in the wastewater likely
295 consumed a portion of the $^{\bullet}OH$ produced.[13,36,66] It is likely that nitrite not only produced, but also
296 scavenged the $^{\bullet}OH$ (k = 1.1 x 10^{10} $M^{-1}s^{-1}$).[13,37]

297 **Table 1.** Steady-state Hydroxyl Radical Concentrations[a]

Nitrogen-containing Matrix	**$[^{\bullet}OH]_{ss,\,280}$ (M)**	**$[^{\bullet}OH]_{ss,\,220}$ (M)**
Synthetic	$8.48\pm0.27\times10^{-15}$	$3.76\pm0.85\times10^{-14}$
Wastewater	$8.69\pm0.30\times10^{-15}$	$3.24\pm0.84\times10^{-14}$

[a]Errors are 95% confidence intervals

298

299 Pharmaceutical compounds were photolyzed at $\lambda \geq 280$, under conditions where direct
300 photolysis was limited and indirect processes dominated (Figure 1). The degradation of the
301 pharmaceuticals was enhanced in the two nitrogen-containing matrices relative to the buffer
302 control (Figure 1; pseudo first order rate constants in Table S4a). The indirect photolysis
303 contribution in the two nitrogen-containing matrices was estimated (Equation 6); it was
304 determined that indirect photolysis was responsible for approximately 76% (synthetic) to 80%
305 (wastewater) of the fluoxetine loss; 90% of the carbamazepine loss (both matrices); 84%
306 (wastewater) to 85% (synthetic) of the trimethoprim loss; and 87% (synthetic) to 91%
307 (wastewater) of the atenolol loss.

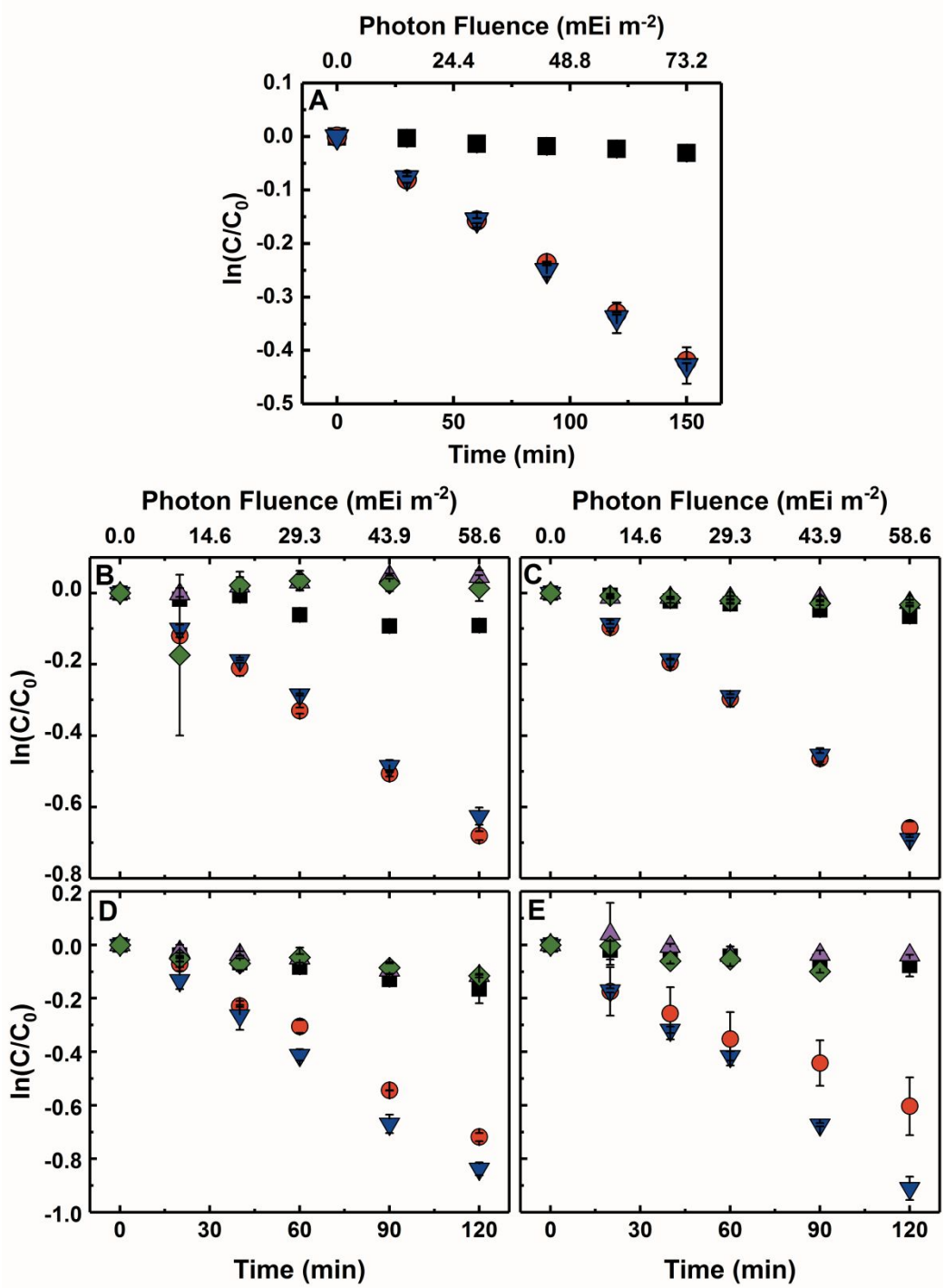

Figure 1. *para*-Chlorobenzoic acid (pCBA) and pharmaceutical compound photodegradation at $\lambda \geq 280$ nm as a function of time and corresponding UV fluence in buffer (black, ■), synthetic nitrogen-containing matrix (red, ●), synthetic nitrogen-containing matrix with IPA added (purple, ▲), nitrogen-containing wastewater matrix (blue, ▼), and nitrogen-containing wastewater matrix with IPA (green, ◆). Panels are: (A) pCBA, (B) trimethoprim, (C) carbamazepine, (D) fluoxetine, and (E) atenolol. Error bars represent one standard deviation of duplicates.

316
317 Reaction by indirect photolysis is attributed to reactions between $^{\bullet}OH$ and the
318 pharmaceuticals. As seen in Figure 1, the addition of IPA (a $^{\bullet}OH$ (and $CO_3^{\bullet-}$) quencher) to the
319 nitrogen-containing matrices significantly slowed the reaction kinetics. This indicates that much
320 of the loss seen beyond direct photolysis (observed in the buffer control) was a result of $^{\bullet}OH$
321 production/reaction. For fluoxetine and atenolol, degradation rates were faster in the wastewater
322 compared to the synthetic nitrogen-containing matrix, but the addition of IPA to both matrices
323 decreased the rate of pharmaceutical degradation to about that observed in the buffer control.
324 Lam et al.[8] found that $CO_3^{\bullet-}$ could play a role in fluoxetine degradation, though oxidation with
325 $^{\bullet}OH$ was likely dominant. Research on the indirect photolysis of atenolol has suggested that
326 reactions can occur with $CO_3^{\bullet-}$, albeit at slower rates compared to those with $^{\bullet}OH$.[12] Conversely,
327 others suggested that $^{\bullet}OH$ was not a major sink for atenolol, whereas reactions with singlet
328 oxygen and triplet excited states were important.[35,69] Our results, however, support the
329 importance of $^{\bullet}OH$ reactions with fluoxetine and atenolol in these nitrite-containing matrices.[11]
330 Experimental bimolecular rate constants for reaction of each pharmaceutical with $^{\bullet}OH$ were
331 determined and are presented in Table 2. The calculated second order rate constants are
332 consistent with a range of literature values collected under various conditions,[8,9,14–16,18,70,71] again
333 indicating that $^{\bullet}OH$ was the primary reactive species in the system.
334
335
336
337
338

339 **Table 2.** Second-order rate constants for reaction with hydroxyl radical in the nitrogen-
340 containing synthetic matrix and wastewater[a]

	λ ≥ 280 nm		λ ≥ 220 nm		
	Synthetic matrix	Wastewater	Synthetic matrix	Wastewater	
Compound	$k_{\bullet OH}$ ($M^{-1}s^{-1}$)	$k_{\bullet OH}$ ($M^{-1}s^{-1}$)	$k_{\bullet OH}$ ($M^{-1}s^{-1}$)	$k_{\bullet OH}$ ($M^{-1}s^{-1}$)	Literature values ($M^{-1}s^{-1}$)
Carbamazepine	$9.34\pm 0.60\times10^9$	$9.23\pm1.01\times10^9$	$6.20\pm1.41\times10^9$	$7.05\pm1.83\times10^9$	$3 – 10\times10^9$ [9,14,15,18,70]
Trimethoprim	$9.39\pm0.60\times10^9$	$8.32\pm0.73\times10^9$	$5.46\pm1.28\times10^9$	$6.04\pm1.62\times10^9$	$6 – 8\times10^9$ [16,18]
Fluoxetine	$8.68\pm0.99\times10^9$	$1.08\pm0.07\times10^{10}$	N/A	N/A	$8 – 10\times10^9$ [8,18]
Atenolol	$8.94\pm1.37\times10^9$	$1.31\pm0.08\times10^{10}$	$3.53\pm1.30\times10^9$	$6.83\pm1.78\times10^9$	$7 – 8\times10^9$ [16,18,71]

[a]Errors are 95% confidence intervals
341

342 *Photolysis reactions in nitrogen-containing wastewater matrices at λ ≥220 nm*

343 As with the experiments at λ ≥ 280 nm, pCBA degradation was assessed at λ ≥ 220 nm to
344 clarify the roles of direct and indirect photolysis, light screening, and •OH in the nitrogen-
345 containing matrices. The degradation of pCBA exhibited pseudo first-order kinetics for λ ≥ 220
346 experiments. Direct photolysis of pCBA occurred as a result of light absorption by pCBA
347 between 220 and 260 nm (Figure S1). The rate of pCBA photolysis at wavelengths above 220
348 nm in buffer was faster than that observed in matrices containing nitrite, however, indicating
349 light screening, and a subsequent slowing of direct photolysis by constituents in the nitrogen-
350 containing matrices occurred (Figure 2, Table S4b). pCBA photolysis was also performed with
351 1% IPA amendment to assess the role of •OH in the system. Because IPA might also quench the
352 direct photolysis process of pCBA if a radical intermediate is involved, a buffer control with IPA
353 and pCBA was also run. Results (Figure 2A) showed that IPA reduced the direct photolysis rate
354 constant of pCBA by 37% ($2.96\pm0.16 \times 10^{-2}$ min^{-1}) in the buffer control, which could indicate
355 quenching of a radical back to the parent compound. The pseudo first-order rate constant for
356 pCBA degradation in buffer with IPA, after correcting for screening (following previously
357 established methods[72,73] described in the ESI), were comparable to the values observed in the

358 nitrogen-containing matrices, suggesting that direct photochemical degradation could account for
359 some of the pCBA loss observed in the nitrogen-containing matrices under the tested conditions.
360 When IPA was added to the nitrogen-containing matrices, however, the reaction slowed
361 dramatically (Figure 2A), with the pseudo first-order rate of pCBA loss in the IPA-quenched
362 experiment ($5.10 \pm 2.50 \times 10^{-3}$ min^{-1}) about 69% lower than in the unquenched analogue (Table SI
363 4b). Taken together, these results corroborate that direct photolysis was effectively screened in
364 the nitrogen-containing matrices, with screening factor calculations (Table S5) suggesting that
365 the matrices screen more than half of light (Figure 2, Table S4b). Loss of pCBA in the nitrogen-
366 containing matrices, therefore, is treated as a reaction with predominantly $^{\bullet}OH$, with direct
367 photolysis minimal in these matrices due to light screening, and the $[^{\bullet}OH]_{ss}$ reported in Table 1 is
368 an upper bound estimate in the system.

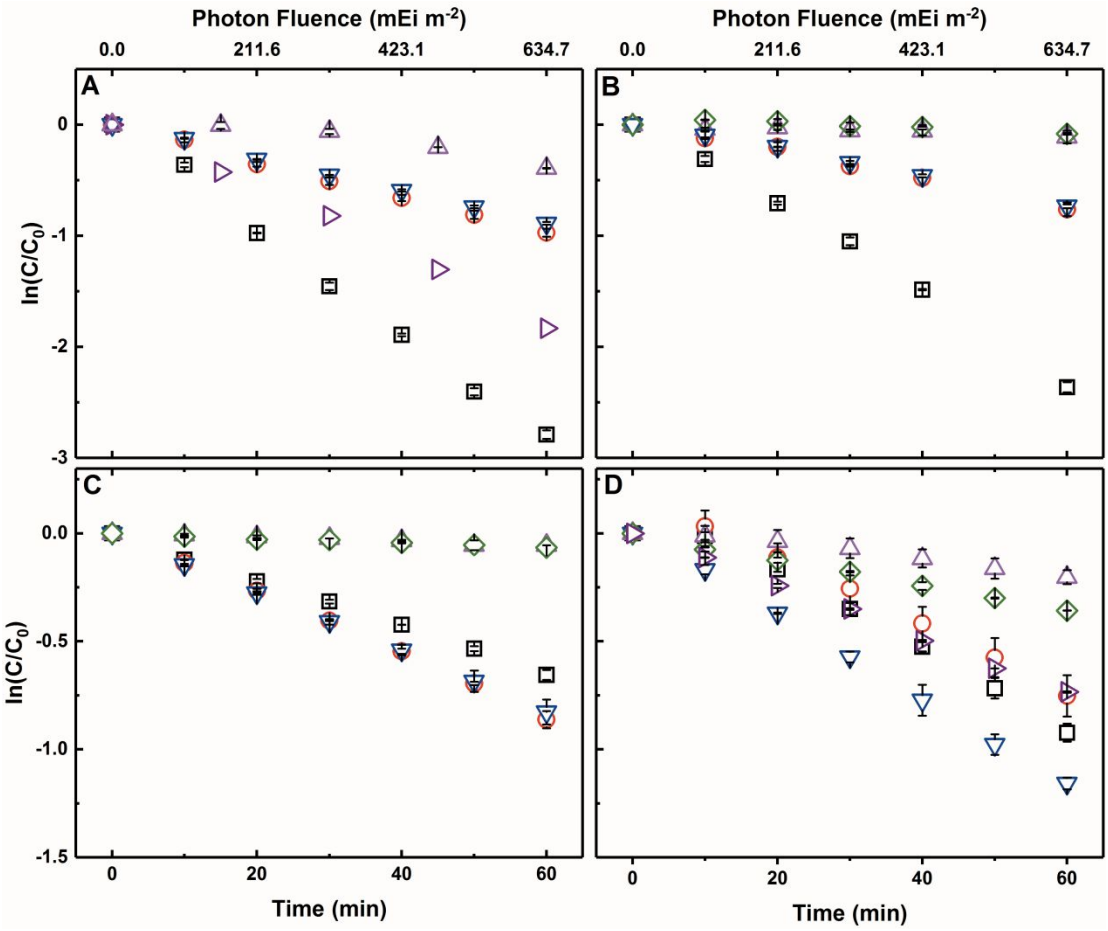

Figure 2. pCBA and pharmaceutical compound photodegradation at $\lambda \geq 220$ nm as a function of time and corresponding UV fluence in buffer (black, □), buffer with IPA (dark purple, ▷), synthetic nitrogen-containing matrix (red, ○), synthetic nitrogen-containing matrix with IPA (purple, △), nitrogen-containing wastewater (blue, ▽), and nitrogen-containing wastewater with IPA (green, ◇). Panels are: (A) pCBA, (B) trimethoprim, (C) carbamazepine, and (D) atenolol. Photolysis of fluoxetine occurred rapidly with complete disappearance within a few minutes; therefore, the data is not shown. Error bars represent one standard deviation of duplicates.

In the case of the pharmaceuticals, both direct and indirect photolysis were also observed, with the degradation of each pharmaceutical faster by an order of magnitude or more when photolyzed under $\lambda \geq 220$ nm conditions (Table S4b). Indeed, at these lower wavelengths the pharmaceuticals experienced significantly enhanced direct photolysis in the solutions without nitrogen. For example, photolysis of fluoxetine under $\lambda \geq 220$ conditions occurred so rapidly that

complete disappearance was observed within a few minutes (data not shown). Trimethoprim exhibited substantial direct photolysis in buffer, and the reaction occurred faster than in the nitrogen-containing matrices, even after accounting for screening. Similar to pCBA, estimated screening factors indicated light screening occurred in the nitrogen-containing matrices, limiting the direct photolysis. IPA quenched the reactions in these matrices, almost completely so for carbamazepine and trimethoprim and approximately 69-72% for atenolol (Figure 2). Thus, like for pCBA, light was absorbed by nitrite and other constituents in the synthetic and wastewater matrices, and direct photolysis was inhibited by light screening in these nitrogen-containing matrices.

Bimolecular rate constants for reaction of carbamazepine and trimethoprim with $^{\bullet}$OH were again estimated (Table 2) as described previously in equation 5, with the exception that k'_{direct} was considered negligible (due to screening as outlined above) and thus $k'_{indirect} = k'_{nitrogen-containing}$. Calculation of bimolecular rate constants for atenolol was more complex. As discussed for the 280 nm conditions, atenolol is known to react with transient oxidants other than $^{\bullet}$OH, such as $CO_3^{\bullet-}$, singlet oxygen, and triplet state organic matter. The experimental results presented herein, however, indicated that while other processes are occurring that are responsible for the partial sensitized degradation of atenolol, $^{\bullet}$OH is the major oxidant in the matrices. To better estimate the rate of indirect photolysis due to $^{\bullet}$OH in the nitrogen-containing matrices, the pseudo first-order rate constants for the IPA spiked experiments were subtracted from the pseudo first-order rate constants of atenolol loss in the respective matrix (i.e., $k'_{indirect,OH} = k'_{nitrogen-containing} - k'_{nitrogen-containing,IPA}$). Overall, the estimates of rate constants for reaction with $^{\bullet}$OH at $\lambda \geq 220$ nm (Table 2) are within approximately a factor of 2 of the values calculated at $\lambda \geq 280$ nm and consistent with literature

values, indicating an important role for •OH in the $\lambda \geq 220$ nm experiments. Thus, while there is inherent error in these calculations due to the uncertainties associated with the steady-state [•OH] estimate and assumptions made based on quencher experiment results, the values appear to be reasonable. We suspect the generally lower values of the second-order rate constants calculated for $\lambda \geq 220$ compared to the experiments at $\lambda \geq 280$ nm and literature values are due to these assumptions.

N-Nitrosamine formation potential

TONO were detected in the nitrogen-containing wastewater at average concentrations ranging from 467.2±31.8 ng/L as NDMA for $\lambda \geq 220$ to 3332.0±72.7 ng/L as NDMA for $\lambda \geq 280$ (Figure 3) at corresponding fluences of $1269.3\ mEi\ m^{-2}$ ($47938.3\ mJ\ cm^{-2}$) to $58.6\ mEi\ m^{-2}$ ($2033.1\ mJ\ cm^{-2}$), respectively. The trace levels of pharmaceuticals studied in these experiments (1 μM of each of the four compounds), some of which contain secondary amine groups, did not increase TONO concentration (349.1±15.4 and 3310.6±14.6 ng/L as NDMA for $\lambda \geq 220$ nm and $\lambda \geq 280$ nm, respectively). TONO concentrations in the dark controls were below the LOQ (10 ng/L as NDMA). The significantly lower TONO concentrations in the nitrogen-containing wastewater irradiated at $\lambda \geq 220$ nm was attributed to greater subsequent photolytic removal of nitrosamines via direct photolysis compared to $\lambda \geq 280$ nm. Due to the relatively high nitrite concentrations and possible microbiologically-derived organic nitrogen in the reactor effluent, the measured TONO concentrations were comparable to, or higher than, levels measured in raw (403-963 ng/L as NDMA), chloraminated (889-2110 ng/L as NDMA), and ozonated (910-2980 ng/L as NDMA) conventional (i.e., no nutrient removal) wastewater effluents.[49]

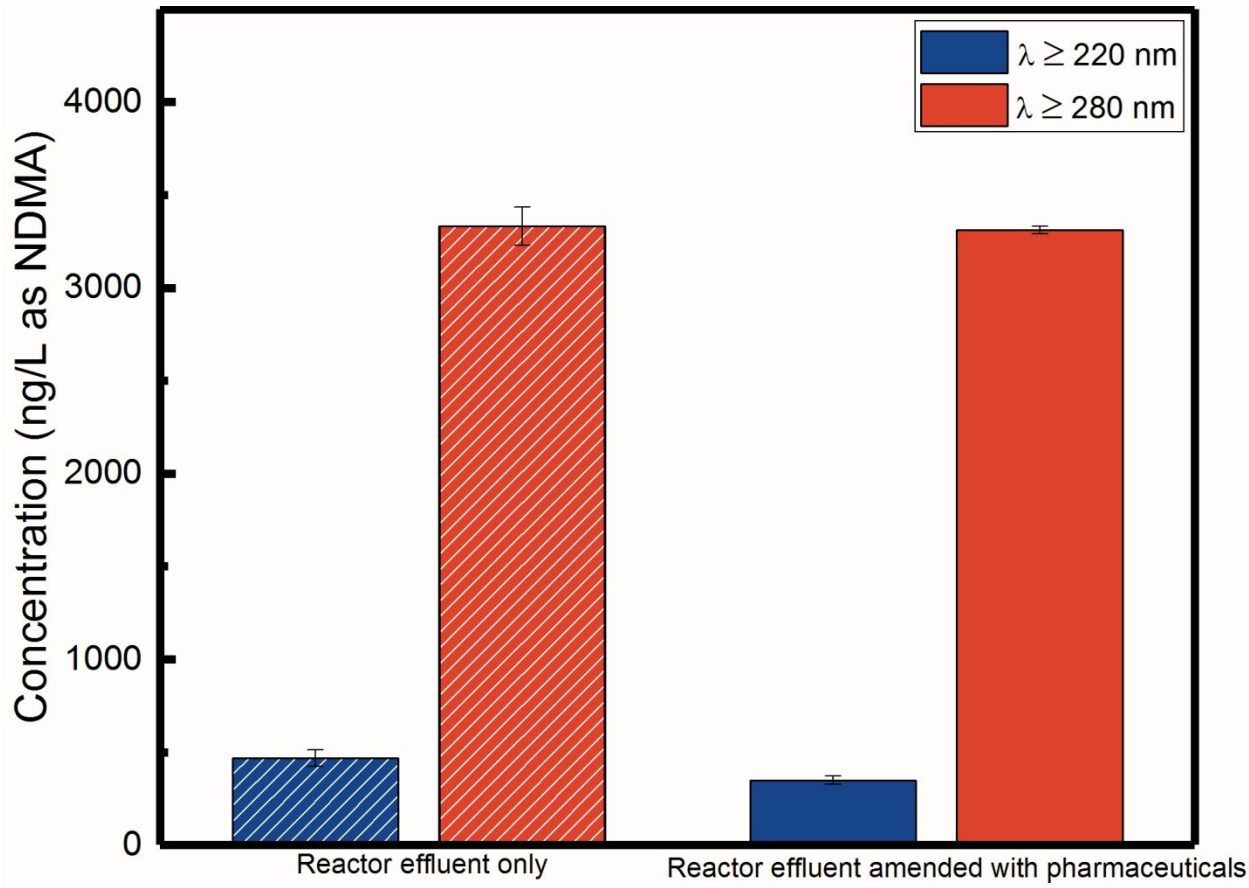

Figure 3. Total nitrosamines in amended reactor effluent samples (n=2) without and with the addition of all four pharmaceutical compounds (1 μM of each) irradiated with the 220 or 280 nm cut-off filter. Error bars represent one standard deviation.

While NDMA is only a fraction of TONO measured in wastewaters,[68,74] for the purposes of modeling a "worst-case" scenario, it is assumed that all nitrosamines formed are NDMA. A first-order linear ordinary differential equation (7) was used to model NDMA concentration as a function of time throughout the reaction vessel. The rate of formation (R_{NDMA}) was based on the photochemical formation of NDMA as a function of dimethylamine and nitrite ion photolysis,[47] minus the rate of subsequent NDMA destruction by direct UV photolysis (k_{loss}).

$$\frac{dC_{NDMA}}{dt} = k_{form}[NO_2^-][DMA] - \phi I_\lambda \varepsilon C_{NDMA} \quad (7)$$

$$\frac{dC_{NDMA}}{dt} = R_{NDMA} - k_{loss}C_{NDMA} \quad (8)$$

$$C_{NDMA}(t) = \frac{R_{NDMA}}{k_{loss}} + \alpha e^{-k_{loss}t} \quad (9)$$

The term α is a constant of integration found using the initial condition $C_{NDMA}(t = 0) = 0$, as shown in equation 9, and is calculated for each model scenario (equation10).

$$\alpha = \frac{-R_{NDMA}}{k_{loss}} \quad (10)$$

Past research has shown that $^{\bullet}$OH does not enhance the photodegradation of NDMA under polychromatic irradiation and that AOPs generating $^{\bullet}$OH are less efficient compared to UV photolysis due to moderate second order rate constants.[53,75] Furthermore, research has suggested that direct photolysis of NDMA dominated under natural sunlight in a wetland system.[12] Subsequently, NDMA loss as a result of reaction with $^{\bullet}$OH was not included in this model for $\lambda \geq 280$ nm and $\lambda \geq 220$ nm conditions.

Eight scenarios were modeled with R_{NDMA} values derived from results reported by Lee and Yoon[47] during the photolysis of 1 mM NO_2^- with either 1 or 4 mM of DMA (i.e., R_{NDMA} for scenario 1 is for 1 mM DMA, $R_{NDMA}$for scenario 2 is for 4 mM DMA, and so on). It was determined that within the first 60 minutes of UV-A (300-400 nm) irradiation with a measured incident photon intensity of 1.4×10^{-5} Einstein $L^{-1}s^{-1}$, 1.26×10^4 ng/L (1.7×10^{-7} M) and 4.59×10^4 ng/L (6.2×10^{-7} M) of NDMA formed with 1 and 4 mM DMA present, respectively.[47] For each scenario, k_{loss} varied and was based on data collected from the TONO measurements in the system presented above (Figure 3) and literature values. The rate of NDMA loss was calculated for scenarios 1-6 using equation 11 and assuming that a steady-state concentration of NDMA ($C_{NDMA,SS}$) would be reached in the system, based on literature observations[47].

$$k_{loss} = \frac{R_{NDMA}}{C_{NDMA,SS}} \quad (11)$$

In scenarios 1 and 2, k_{loss} was derived using the approximate $C_{NDMA,SS}$ from Lee and Yoon; approximate steady-state concentrations of NDMA at 180 minutes were estimated to be 1.11×10^4 ng/L (1.5×10^{-7} M) and 4.44×10^4 ng/L (6.0×10^{-7} M) for 1 and 4 mM DMA respectively. In scenarios 3 – 6, measured TONO concentrations in reactor samples irradiated under conditions of $\lambda \geq 220$ nm and $\lambda \geq 280$ nm were used to estimate k_{loss} values in our system. Because the measurements were made after 120 minutes of irradiation, it was assumed the concentration of TONO had reached steady state, and that concentration was treated as the equivalent steady state NDMA concentration. In scenarios 7 and 8, a time-based, average k_{loss} $(= 0.36\ min^{-1})$ from Sharpless and Linden[53] for direct photochemical reaction between 200 and 300 nm was used.

UV fluences above 500 mJ cm^{-2} were used for NDMA removal[53] and a fluence of ~1000 mJ cm^{-2} was required for a log order reduction in NDMA[45]. For all scenarios modeled (Figure 4) significant steady-state concentrations of NDMA formed over 120 minutes, assuming minimal destruction of nitrosamine precursors throughout irradiation. For scenarios 5 and 6, which exhibited the lowest steady-state concentrations, even with polychromatic light irradiation at $\lambda \geq$ 220 nm for 30 minutes – an equivalent fluence of $317.3\ mEi\ m^{-2}$ $(11984.6\ mJ\ cm^{-2})$, the model predicted NDMA concentrations reaching about 467 ng/L as NDMA.

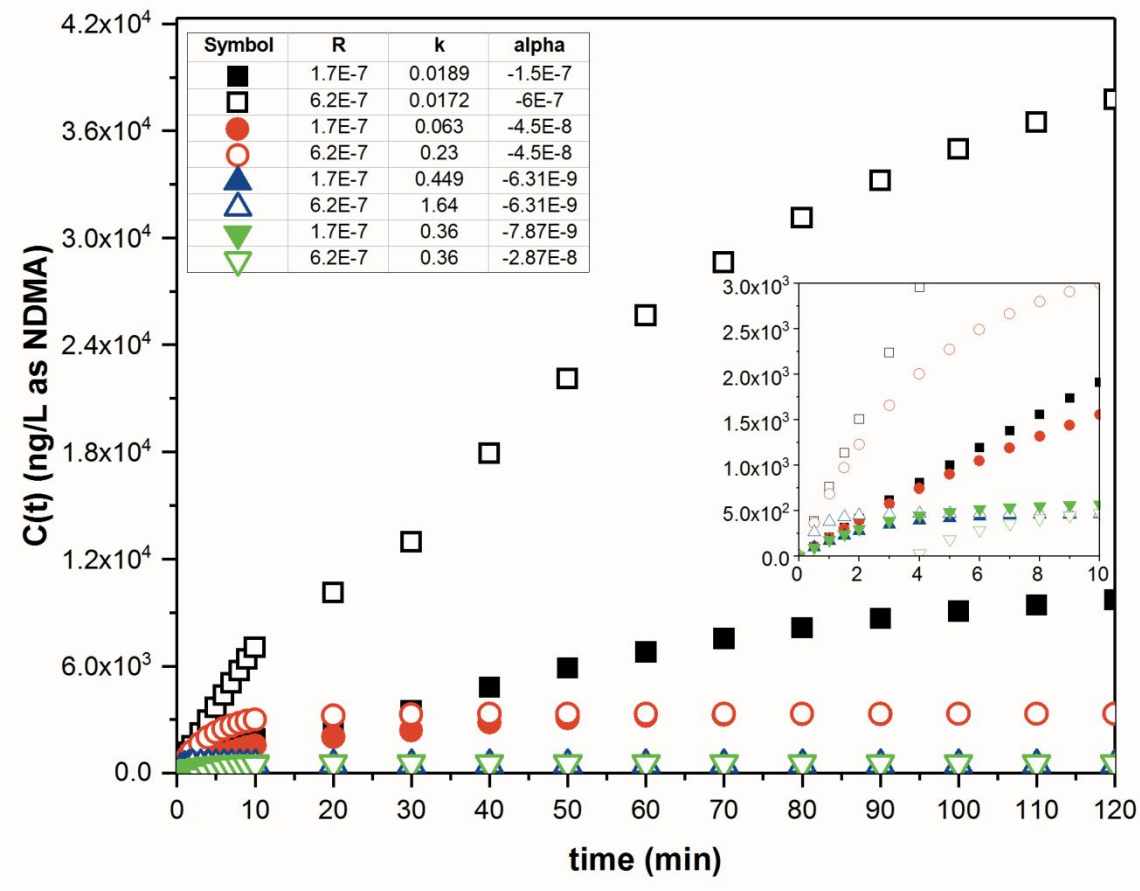

Figure 4. Model of NDMA concentrations over time for 8 scenarios. Symbols and corresponding model variables, rate of formation (*R*, M min^{-1}), rate constant of loss (*k,* min^{-1}), and constant of integration (*alpha*), are summarized in the inset table in the left corner of the figure. Rates of formation are a function of either 4 mM (indicated by open symbols) or 1 mM DMA (indicated by closed symbols) and 1 mM nitrite for λ = 300-400 nm. Scenarios 1 and 2 are represented by squares (□,■) with rates of loss calculated from Lee and Yoon 2007[47] for λ = 300-400 nm; scenarios 3 and 4 are represented by circles (○,●) with rates of loss calculated from reactor effluent λ ≥ 280 nm TONO measurements (Figure 3); scenarios 5 and 6 are represented by triangles (△,▲) with rates of loss calculated from reactor effluent λ ≥ 220 nm TONO measurements (Figure 3); scenarios 7 and 8 are represented by upside down triangles (▼,▽) with the rate of loss constant determined by Sharpless and Linden 2003[53].

Conclusions

In a partially nitritated wastewater stream containing high levels of nitrite, trace pharmaceutical compounds could undergo photolytic degradation when exposed to UV. The results of this study also suggest that if nitritated effluents were exposed to solar light (for

example, in a treatment wetland or lagoon), trace organic contaminants would also be degraded by solar photolysis. Oxidation by $^{\bullet}OH$ was responsible for much of the degradation observed. This process could increase removal of organic contaminants found in municipal wastewater, in particular, compounds that are considered recalcitrant because they are not readily biodegraded or completely removed by conventional or anaerobic treatment and may have low direct photolysis quantum yields. Previous research has shown that some recalcitrant pharmaceuticals, such as carbamazepine, and their products can undergo enhanced biotransformation and mineralization after UV/H_2O_2 AOP treatment and antibiotics like trimethoprim can have no antibacterially active transformation products.[76–78] Therefore, transformation of these compounds by reaction with $^{\bullet}OH$ could increase the susceptibility of products to biodegradation, which would make an intermediate UV process even more promising to further remove these trace organic compounds, especially those that already demonstrate some propensity to biodegrade.[25,26,76,79–81] Nevertheless, a foreseeable downside is that significant total N-nitrosamine formation could occur from nitrite photolysis. Because nitrosamines are also subject to photolytic degradation, more research is needed to determine how to operate such a system to facilitate nitrosamine loss in addition to pharmaceutical destruction.

Conflicts of Interest

The authors declare no conflicts of interest.

Acknowledgements

The authors acknowledge funding provided by the University of Minnesota, NSF Sustainability Research Networks grant (1444745), and the Environment and Natural Resources

Trust Fund as recommended by the Legislative Citizen Commission on Minnesota Resources. We would like to thank Kira Peterson and J. Cesar Bezares-Cruz for help with reactor set-up, operation, and maintenance, Teng Zeng and Chancheng Pu at Syracuse University for performing the TONO analyses, and Griffin Dempsey for assistance with laboratory work.

References

1 I. Michael, L. Rizzo, C. S. McArdell, C. M. Manaia, C. Merlin, T. Schwartz, C. Dagot and D. Fatta-Kassinos, Urban wastewater treatment plants as hotspots for the release of antibiotics in the environment: A review, *Water Res.*, 2013, **47**, 957–995.

2 R. L. Oulton, T. Kohn and D. M. Cwiertny, Pharmaceuticals and personal care products in effluent matrices: A survey of transformation and removal during wastewater treatment and implications for wastewater management, *J. Environ. Monit.*, 2010, **12**, 1956.

3 B. Petrie, R. Barden and B. Kasprzyk-Hordern, A review on emerging contaminants in wastewaters and the environment: Current knowledge, understudied areas and recommendations for future monitoring, *Water Res.*, 2014, **72**, 3–27.

4 S. A. Snyder, P. Westerhoff, Y. Yoon and D. L. Sedlak, Pharmaceuticals, Personal Care Products, and Endocrine Disruptors in Water: Implications for the Water Industry, *Environ. Eng. Sci.*, 2003, **20**, 449–469.

5 M. Clara, B. Strenn and N. Kreuzinger, Carbamazepine as a possible anthropogenic marker in the aquatic environment: investigations on the behaviour of Carbamazepine in wastewater treatment and during groundwater infiltration, *Water Res.*, 2004, **38**, 947–954.

6 R. I. L. Eggen, J. Hollender, A. Joss, M. Schärer and C. Stamm, Reducing the Discharge of Micropollutants in the Aquatic Environment: The Benefits of Upgrading Wastewater

Treatment Plants, *Environ. Sci. Technol.*, 2014, **48**, 7683–7689.

7 M. W. Lam, C. J. Young, R. A. Brain, D. J. Johnson, M. A. Hanson, C. J. Wilson, S. M. Richards, K. R. Solomon and S. A. Mabury, Aquatic persistence of eight pharmaceuticals in a microcosm study., *Environ. Toxicol. Chem.*, 2004, **23**, 1431–40.

8 M. W. Lam, C. J. Young and S. A. Mabury, Aqueous Photochemical Reaction Kinetics and Transformations of Fluoxetine, *Environ. Sci. Technol.*, 2005, **39**, 513–522.

9 M. W. Lam and S. A. Mabury, Photodegradation of the pharmaceuticals atorvastatin, carbamazepine, levofloxacin, and sulfamethoxazole in natural waters, *Aquat. Sci.*, 2005, **67**, 177–188.

10 S. Chiron, C. Minero and D. Vione, Photodegradation processes of the antiepileptic drug carbamazepine, relevant to estuarine waters, *Environ. Sci. Technol.*, 2006, **40**, 5977–5983.

11 C. Zeng, Y. Ji, L. Zhou, Y. Zhang and X. Yang, The role of dissolved organic matters in the aquatic photodegradation of atenolol, *J. Hazard. Mater.*, 2012, **239**–**240**, 340–347.

12 J. T. Jasper and D. L. Sedlak, Phototransformation of wastewater-derived trace organic contaminants in open-water unit process treatment wetlands, *Environ. Sci. Technol.*, 2013, **47**, 10781–10790.

13 O. S. Keen, N. G. Love and K. G. Linden, The role of effluent nitrate in trace organic chemical oxidation during UV disinfection, *Water Res.*, 2012, **46**, 5224–5234.

14 V. J. Pereira, H. S. Weinberg, K. G. Linden and P. C. Singer, UV Degradation Kinetics and Modeling of Pharmaceutical Compounds in Laboratory Grade and Surface Water via Direct and Indirect Photolysis at 254 nm, *Environ. Sci. Technol.*, 2007, **41**, 1682–1688.

15 V. J. Pereira, K. G. Linden and H. S. Weinberg, Evaluation of UV irradiation for photolytic and oxidative degradation of pharmaceutical compounds in water, *Water Res.*,

2007, **41**, 4413–4423.

16 F. L. Rosario-Ortiz, E. C. Wert and S. A. Snyder, Evaluation of UV/H2O2 treatment for the oxidation of pharmaceuticals in wastewater, *Water Res.*, 2010, **44**, 1440–1448.

17 C. C. Ryan, D. T. Tan and W. A. Arnold, Direct and indirect photolysis of sulfamethoxazole and trimethoprim in wastewater treatment plant effluent, *Water Res.*, 2011, **45**, 1280–1286.

18 B. A. Wols, C. H. M. Hofman-Caris, D. J. H. Harmsen and E. F. Beerendonk, Degradation of 40 selected pharmaceuticals by UV/H2O2, *Water Res.*, 2013, **47**, 5876–5888.

19 H. Gao, Y. D. Scherson and G. F. Wells, Towards energy neutral wastewater treatment: methodology and state of the art, *Environ. Sci. Process. Impacts*, 2014, **16**, 1223–1246.

20 M. Jetten, M. Schmid, K. Van De Pas-Schoonen, J. S. Damsté and M. Strous, Anammox organisms: Enrichment, cultivation, and environmental analysis, *Methods Enzymol.*, 2005, **397**, 34–57.

21 J. G. Kuenen, Anammox bacteria: from discovery to application, *Nat Rev Microbiol*, 2008, **6**, 320–326.

22 S. Lackner, E. M. Gilbert, S. E. Vlaeminck, A. Joss, H. Horn and M. C. M. van Loosdrecht, Full-scale partial nitritation/anammox experiences – An application survey, *Water Res.*, 2014, **55**, 292–303.

23 Y. Cao, M. C. M. van Loosdrecht and G. T. Daigger, Mainstream partial nitritation–anammox in municipal wastewater treatment: status, bottlenecks, and further studies, *Appl. Microbiol. Biotechnol.*, 2017, **101**, 1365–1383.

24 J. Delgado Vela, L. B. Stadler, K. J. Martin, L. Raskin, C. B. Bott and N. G. Love, Prospects for Biological Nitrogen Removal from Anaerobic Effluents during Mainstream

Wastewater Treatment, *Environ. Sci. Technol. Lett.*, 2015, **2**, 234–244.

25 T. Alvarino, S. Suarez, E. Katsou, J. Vazquez-Padin, J. M. Lema and F. Omil, Removal of PPCPs from the sludge supernatant in a one stage nitritation/anammox process, *Water Res.*, 2015, **68**, 701–709.

26 S. Sathyamoorthy, K. Chandran and C. A. Ramsburg, Biodegradation and cometabolic modeling of selected beta blockers during ammonia oxidation, *Environ. Sci. Technol.*, 2013, **47**, 12835–12843.

27 K. N. Peterson, D. T. Tan, J. C. Bezares-Cruz and P. J. Novak, Estrone biodegradation in laboratory-scale systems designed for total nitrogen removal from wastewater, *Environ. Sci. Water Res. Technol.*, 2017, **3**, 1051–1060.

28 F. L. Rosario-Ortiz and S. Canonica, *Environ. Sci. Technol.*, 2016, 50, 12532–12547.

29 J. Mack and J. R. Bolton, Photochemistry of nitrite and nitrate in aqueous solution: a review, *J. Photochem. Photobiol. A Chem.*, 1999, **128**, 1–13.

30 O. C. Zafiriou and M. B. True, Nitrite photolysis in seawater by sunlight, *Mar. Chem.*, 1979, **8**, 9–32.

31 D. Kim, J. Lee, J. Ryu, K. Kim and W. Choi, Arsenite Oxidation Initiated by the UV Photolysis of Nitrite and Nitrate, *Environ. Sci. Technol.*, 2014, **48**, 4030–4037.

32 P. Calza, D. Vione, A. Novelli, E. Pelizzetti and C. Minero, The role of nitrite and nitrate ions as photosensitizers in the phototransformation of phenolic compounds in seawater, *Sci. Total Environ.*, 2012, **439**, 67–75.

33 M. M. Huber, S. Canonica, G. Y. Park and U. Von Gunten, Oxidation of pharmaceuticals during ozonation and advanced oxidation processes, *Environ. Sci. Technol.*, 2003, **37**, 1016–1024.

34 M. Klavarioti, D. Mantzavinos and D. Kassinos, Removal of residual pharmaceuticals from aqueous systems by advanced oxidation processes, *Environ. Int.*, 2009, **35**, 402–417.

35 L. Wang, H. Xu, W. J. Cooper and W. Song, Photochemical fate of beta-blockers in NOM enriched waters, *Sci. Total Environ.*, 2012, **426**, 289–295.

36 P. L. Brezonik and J. Fulkerson-Brekken, Nitrate-Induced Photolysis in Natural Waters: Controls on Concentrations of Hydroxyl Radical Photo-Intermediates by Natural Scavenging Agents, *Environ. Sci. Technol.*, 1998, **32**, 3004–3010.

37 P. P. Vaughan and N. V. Blough, Photochemical Formation of Hydroxyl Radical by Constituents of Natural Waters, *Environ. Sci. Technol.*, 1998, **32**, 2947–2953.

38 R. G. Zepp, J. Hoigne and H. Bader, Nitrate-induced photooxidation of trace organic chemicals in water, *Environ. Sci. Technol.*, 1987, **21**, 443–450.

39 O. C. Zafiriou and M. B. True, Nitrite photolysis as a source of free radicals in productive surface waters, *Geophys. Res. Lett.*, 1979, **6**, 81–84.

40 R. Andreozzi, M. Raffaele and P. Nicklas, Pharmaceuticals in STP effluents and their solar photodegradation in aquatic environment, *Chemosphere*, 2003, **50**, 1319–1330.

41 C. M. Sharpless and K. G. Linden, UV Photolysis of Nitrate: Effects of Natural Organic Matter and Dissolved Inorganic Carbon and Implications for UV Water Disinfection, *Environ. Sci. Technol.*, 2001, **35**, 2949–2955.

42 C. M. Sharpless, D. A. Seibold and K. G. Linden, Nitrate photosensitized degradation of atrazine during UV water treatment, *Aquat. Sci.*, 2003, **65**, 359–366.

43 A. R. Lado Ribeiro, N. F. F. Moreira, G. Li Puma and A. M. T. Silva, Impact of water matrix on the removal of micropollutants by advanced oxidation technologies, *Chem. Eng. J.*, 2019, **363**, 155–173.

638 44 S. Bahnmüller, U. von Gunten and S. Canonica, Sunlight-induced transformation of
639 sulfadiazine and sulfamethoxazole in surface waters and wastewater effluents, *Water Res.*,
640 2014, **57**, 183–192.
641 45 M. Sgroi, F. G. A. Vagliasindi, S. A. Snyder and P. Roccaro, N-Nitrosodimethylamine
642 (NDMA) and its precursors in water and wastewater: A review on formation and removal,
643 *Chemosphere*, 2018, **191**, 685–703.
644 46 T. Zeng and W. A. Mitch, Impact of Nitrification on the Formation of *N* -Nitrosamines
645 and Halogenated Disinfection Byproducts within Distribution System Storage Facilities,
646 *Environ. Sci. Technol.*, 2016, **50**, 2964–2973.
647 47 C. Lee and J. Yoon, UV-A induced photochemical formation of N-nitrosodimethylamine
648 (NDMA) in the presence of nitrite and dimethylamine, *J. Photochem. Photobiol. A Chem.*,
649 2007, **189**, 128–134.
650 48 T. Zeng and W. A. Mitch, Contribution of *N* -Nitrosamines and Their Precursors to
651 Domestic Sewage by Greywaters and Blackwaters, *Environ. Sci. Technol.*, 2015, **49**,
652 13158–13167.
653 49 T. Zeng, C. M. Glover, E. J. Marti, G. C. Woods-Chabane, T. Karanfil, W. A. Mitch and
654 E. R. V. Dickenson, Relative Importance of Different Water Categories as Sources of *N* -
655 Nitrosamine Precursors, *Environ. Sci. Technol.*, 2016, **50**, 13239–13248.
656 50 K. A. Thorn and L. G. Cox, Ultraviolet Irradiation Effects Incorporation of Nitrate and
657 Nitrite Nitrogen into Aquatic Natural Organic Matter, *J. Environ. Qual.*, 2012, **41**, 865.
658 51 S. W. Krasner, W. A. Mitch, D. L. McCurry, D. Hanigan and P. Westerhoff, *Water Res.*,
659 2013, 47, 4433–4450.
660 52 T. Ohta, J. Suzuki, Y. Iwano and S. Suzuki, Photochemical nitrosation of dimethylamine

661 in aqueous solution containing nitrite, *Chemosphere*, 1982, **11**, 797–801.
662 53 C. M. Sharpless and K. G. Linden, Experimental and Model Comparisons of Low- and
663 Medium-Pressure Hg Lamps for the Direct and H 2 O 2 Assisted UV Photodegradation of
664 N -Nitrosodimethylamine in Simulated Drinking Water, *Environ. Sci. Technol.*, 2003, **37**,
665 1933–1940.
666 54 M. J. Benotti, R. A. Trenholm, B. J. Vanderford, J. C. Holady, B. D. Stanford and S. A.
667 Snyder, Pharmaceuticals and Endocrine Disrupting Compounds in U.S. Drinking Water,
668 *Environ. Sci. Technol.*, 2009, **43**, 597–603.
669 55 E. T. Furlong, A. L. Batt, S. T. Glassmeyer, M. C. Noriega, D. W. Kolpin, H. Mash and
670 K. M. Schenck, Nationwide reconnaissance of contaminants of emerging concern in
671 source and treated drinking waters of the United States: Pharmaceuticals, *Sci. Total*
672 *Environ.*, 2017, **579**, 1629–1642.
673 56 M. S. Kostich, A. L. Batt and J. M. Lazorchak, Concentrations of prioritized
674 pharmaceuticals in effluents from 50 large wastewater treatment plants in the US and
675 implications for risk estimation, *Environ. Pollut.*, 2014, **184**, 354–359.
676 57 J. M. Burns, W. J. Cooper, J. L. Ferry, D. W. King, B. P. DiMento, K. McNeill, C. J.
677 Miller, W. L. Miller, B. M. Peake, S. A. Rusak, A. L. Rose and T. D. Waite, Methods for
678 reactive oxygen species (ROS) detection in aqueous environments, *Aquat. Sci.*, 2012, **74**,
679 683–734.
680 58 S. Canonica, L. Meunier and U. von Gunten, Phototransformation of selected
681 pharmaceuticals during UV treatment of drinking water, *Water Res.*, 2008, **42**, 121–128.
682 59 V. Kouba, D. Vejmelkova, E. Proksova, H. Wiesinger, M. Concha, P. Dolejs, J. Hejnic, P.
683 Jenicek and J. Bartacek, High-Rate Partial Nitritation of Municipal Wastewater after

Psychrophilic Anaerobic Pretreatment, *Environ. Sci. Technol.*, 2017, acs.est.7b02078.

60 T. Lotti, R. Kleerebezem, Z. Hu, B. Kartal, M. S. M. Jetten and M. C. M. van Loosdrecht, Simultaneous partial nitritation and anammox at low temperature with granular sludge, *Water Res.*, 2014, **66**, 111–121.

61 J. L. Packer, J. J. Werner, D. E. Latch, K. McNeill and W. A. Arnold, Photochemical fate of pharmaceuticals in the environment: Naproxen, diclofenac, clofibric acid, and ibuprofen, *Aquat. Sci.*, 2003, **65**, 342–351.

62 J. R. Bolton, I. Mayor-Smith and K. G. Linden, Rethinking the Concepts of Fluence (UV Dose) and Fluence Rate: The Importance of Photon-based Units - A Systemic Review, *Photochem. Photobiol.*, 2015, **91**, 1252–1262.

63 J. M. Barazesh, T. Hennebel, J. T. Jasper and D. L. Sedlak, Modular Advanced Oxidation Process Enabled by Cathodic Hydrogen Peroxide Production, *Environ. Sci. Technol.*, 2015, **49**, 7391–7399.

64 P. Neta, P. Maruthamuthu, P. M. Carton and R. W. Fessenden, Formation and reactivity of the amino radical, *J. Phys. Chem.*, 1978, **82**, 1875–1878.

65 P. Neta, R. E. Huie and A. B. Ross, Rate Constants for Reactions of Inorganic Radicals in Aqueous Solution, *J. Phys. Chem. Ref. Data*, 1988, **17**, 1027–1284.

66 G. V. Buxton, C. L. Greenstock, W. P. Helman and A. B. Ross, Critical Review of rate constants for reactions of hydrated electrons, hydrogen atoms and hydroxyl radicals (·OH/·O − in Aqueous Solution, *J. Phys. Chem. Ref. Data*, 1988, **17**, 513–886.

67 P. Kulshrestha, K. C. McKinstry, B. O. Fernandez, M. Feelisch and W. A. Mitch, Application of an optimized total N -nitrosamine (TONO) assay to pools: Placing N -nitrosodimethylamine (NDMA) determinations into perspective, *Environ. Sci. Technol.*,

2010, **44**, 3369–3375.

68 N. Dai, T. Zeng and W. A. Mitch, Predicting N-nitrosamines: N-nitrosodiethanolamine as a significant component of total N-nitrosamines in recycled wastewater, *Environ. Sci. Technol. Lett.*, 2015, **2**, 54–58.

69 M. M. Dong, R. Trenholm and F. L. Rosario-Ortiz, Photochemical degradation of atenolol, carbamazepine, meprobamate, phenytoin and primidone in wastewater effluents, *J. Hazard. Mater.*, 2015, **282**, 216–223.

70 Z. Shu, J. R. Bolton, M. Belosevic and M. Gamal El Din, Photodegradation of emerging micropollutants using the medium-pressure UV/H2O2 Advanced Oxidation Process, *Water Res.*, 2013, **47**, 2881–2889.

71 W. Song, W. J. Cooper, S. P. Mezyk, J. Greaves and B. M. Peake, Free Radical Destruction of β-Blockers in Aqueous Solution, *Environ. Sci. Technol.*, 2008, **42**, 1256–1261.

72 M. E. Karpuzcu, A. J. McCabe and W. A. Arnold, Phototransformation of pesticides in prairie potholes: effect of dissolved organic matter in triplet-induced oxidation, *Environ. Sci. Process. Impacts*, 2016, **18**, 237–245.

73 A. J. McCabe and W. A. Arnold, Reactivity of Triplet Excited States of Dissolved Natural Organic Matter in Stormflow from Mixed-Use Watersheds, *Environ. Sci. Technol.*, 2017, **51**, 9718–9728.

74 N. Dai and W. A. Mitch, Relative Importance of N -Nitrosodimethylamine Compared to Total N -Nitrosamines in Drinking Waters, *Environ. Sci. Technol.*, 2013, **47**, 3648–3656.

75 D. B. Miklos, C. Remy, M. Jekel, K. G. Linden, J. E. Drewes and U. Hübner, Evaluation of advanced oxidation processes for water and wastewater treatment – A critical review,

Water Res., 2018, **139**, 118–131.

76 O. S. Keen, S. Baik, K. G. Linden, D. S. Aga and N. G. Love, Enhanced Biodegradation of Carbamazepine after UV/H 2 O 2 Advanced Oxidation, *Environ. Sci. Technol.*, 2012, **46**, 6222–6227.

77 O. S. Keen and K. G. Linden, Degradation of Antibiotic Activity during UV/H_2O_2 Advanced Oxidation and Photolysis in Wastewater Effluent, *Environ. Sci. Technol.*, 2013, **47**, 13020–13030.

78 O. S. Keen, N. G. Love, D. S. Aga and K. G. Linden, Biodegradability of iopromide products after UV/H2O2 advanced oxidation, *Chemosphere*, 2016, **144**, 989–994.

79 A. L. Batt, S. Kim and D. S. Aga, Enhanced biodegradation of lopromide and trimethoprim in nitrifying activated sludge, *Environ. Sci. Technol.*, 2006, **40**, 7367–7373.

80 V. M. Monsalvo, J. A. McDonald, S. J. Khan and P. Le-Clech, Removal of trace organics by anaerobic membrane bioreactors, *Water Res.*, 2014, **49**, 103–112.

81 A.-K. Ghattas, F. Fischer, A. Wick and T. A. Ternes, Anaerobic biodegradation of (emerging) organic contaminants in the aquatic environment, *Water Res.*, 2017, **116**, 268–295.